

Joule-Thomson Microcryocooler Test Results

**J.R. Olson¹, E. Roth¹, M. Guzinski¹, A. Ruiz¹,
C.L. Mangun², D. King², N. Hejmanowski², D.L. Carroll²**

¹Lockheed Martin Space, Palo Alto, CA 94304

²CU Aerospace, Champaign, IL 61820

ABSTRACT

Small closed-cycle Joule-Thomson (JT) cryocoolers offer certain advantages in packaging and heat rejection when compared with Stirling and pulse tube cryocoolers. This paper describes results of performance testing of a closed-cycle JT microcryocooler. The JT cooler is driven by a 200-gram JT micro compressor developed by Lockheed Martin and previously presented at ICC 19¹. The counterflow heat exchanger was produced by CU Aerospace in Champaign, IL, USA, and is a novel anisotropic material consisting of a woven array of counterflowing microcapillaries and copper isothermalization wires. The microcapillaries are created using a novel sacrificial fiber method and encapsulated in an epoxy matrix using CU Aerospace's VascTech™ process, details of which are presented in this paper. Testing was performed with R14 gas in both open-cycle and closed-cycle cooling modes.

INTRODUCTION AND MOTIVATION

The use of small closed-cycle JT cryocoolers in tactical and space applications has been extremely limited, mainly because of the low JT thermodynamic efficiency at typical cryogenic device temperatures of 80 K. The primary space application for JT cryocoolers is for applications below 6 K using helium JT coolers, such as the MIRI instrument on the James Webb Space Telescope².

Recent advances in mid-wave infrared (MWIR) focal planes allow operation in the range of 125 K to 150 K³, and JT cryocoolers operating at higher temperature can benefit from gas mixtures to potentially achieve efficiencies as high as Stirling-cycle cryocoolers. The primary benefit of using a JT cooler is the potential for compact cooler packaging. Figure 1 shows a photograph of a MWIR camera built by Lockheed Martin Santa Barbara Focal Plane, which includes a state of the art MWIR focal plane packaged with a Lockheed Martin microcryocooler⁴, and the cryocooler coldfinger occupies a significant fraction of the camera volume. Any reduction in the length of the optics, such as that taken up by the coldfinger, reduces the optical path length and degrades camera sensitivity.

CLOSED-CYCLE JT CRYOCOOLER COMPONENTS

The primary components of a closed-cycle JT cryocooler are shown in Figure 2. These include a closed-cycle compressor to provide the high and low pressures required by the JT thermodynamic cycle, a counterflow heat exchanger, and a cold block with the JT constriction.

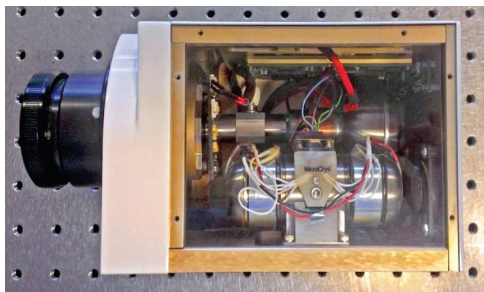


Figure 1. MWIR camera incorporating a Lockheed Martin Microcryocooler

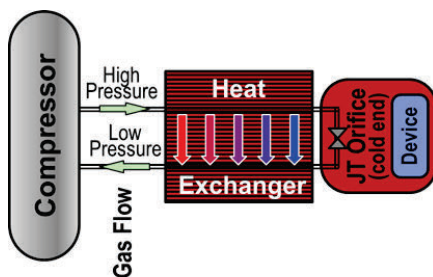


Figure 2. Primary components of a closed-cycle JT Cryocooler.

The closed-cycle JT cooler has the potential to be packaged compactly. Unlike Stirling-cycle coolers, the JT compressor can be located remotely from the coldhead with very little loss in performance, and all the heat can be rejected at the compressor. Furthermore, it is possible to compactly package the JT coldhead, leading to a versatile cooler allowing the maximum optics volume. Figure 3 shows one such JT configuration, where the coldhead and optical window can be seen packaged remotely from the JT compressor.

JT Micro Compressor

The closed-cycle JT compressor, shown in Figure 4 was reported in a previous paper¹. The compressor power efficiency is approximately 25-30%, and a representative example of the compressor performance is shown in Figure 5. The nominal low pressure is 75-100 PSI with a pressure ratio of around 4:1.

Counterflow Heat Exchanger

The counterflow heat exchanger is another important component of the closed-cycle JT cryocooler. This heat exchanger allows the warm high-pressure gas flowing from the warm to the cold end to be cooled by the cold low-pressure gas flowing from the cold to the warm end. The effectiveness of this heat exchanger must be very high to achieve good JT thermodynamic efficiency. The development of a novel counterflow heat exchanger, led by CU Aerospace in Champaign, IL, USA, was the primary task of the project that funded this work. CU Aerospace has commercialized a

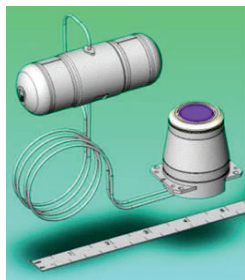


Figure 3. Closed-cycle JT cooler, with the coldhead remotely packaged from the compressor.

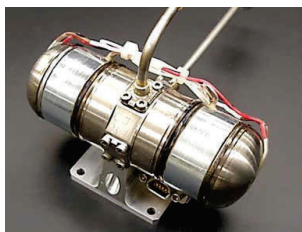


Figure 4. Lockheed Martin closed-cycle JT compressor, with a mass of 200 grams. This compressor performance was previously reported¹.

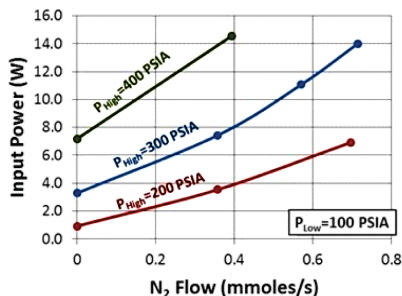


Figure 5. A subset of the measured performance of the JT Microcompressor shown in Figure 4

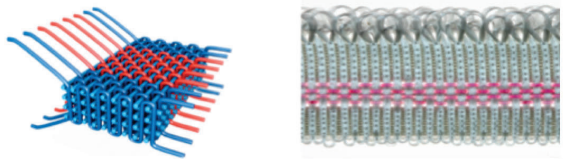


Figure 6a. Sacrificial Fibers (pink) woven with glass fibers.

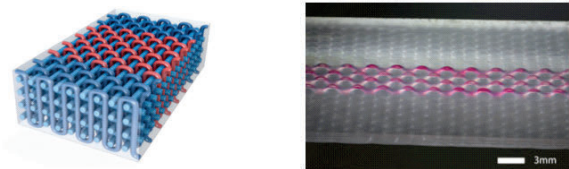


Figure 6b. Woven material infused with epoxy resin using VARTM

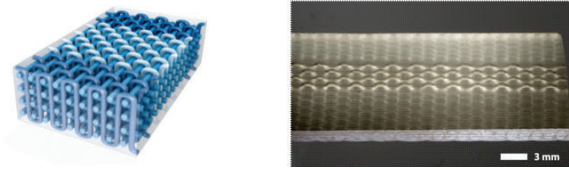


Figure 6c. Fiber evacuation by heating to 200°C for 12 hours under vacuum

sacrificial material manufacturing technique⁵ called vaporization of sacrificial components technology (VascTech) originally developed at the University of Illinois⁶. The technique relies on sacrificial fibers, similar in physical characteristics to fishing line, which can be cast in epoxy using vacuum assisted resin transfer molding (VARTM) and subsequently evaporated, leaving hollow capillary channels within the epoxy. One such weave⁶ is shown in Figure 6, where the pink sacrificial fibers are woven with glass fibers (a), cast in epoxy (b) and evaporated away, leaving channels in the solid material (c).

For this work, sacrificial warp fibers were woven with copper weft wires to create an anisotropic material. This weave is shown in Figure 7, which shows a photograph of the woven material prior to VARTM, the thermally-modeled geometry, and a micrograph of the channels following the VascTech process with a high-contrast fluid inside them. The idea is to alternate high- and low-pressure capillaries, using as many pairs of capillaries as necessary to achieve sufficiently low pressure drop, and relying on the high thermal conductivity and short heat conduction length of the copper wires between alternating channels to exchange heat between the two gas streams.

The as-woven geometry is shown in Figure 8. Unfortunately, a glass warp tow was included during the weave process in between the two copper wires. Heat exchange only effectively takes place where channels bend over copper wire, and the alternating capillaries contact different copper wires, so there is no effective heat exchange between the high- and low-pressure channels. The details of this weave were not understood until late in the project. A correctly-woven sample was hastily produced, but there was leakage between the high- and low-pressure channels, so we were required to test the configuration in Figure 8 knowing the performance and effectiveness would not be good.

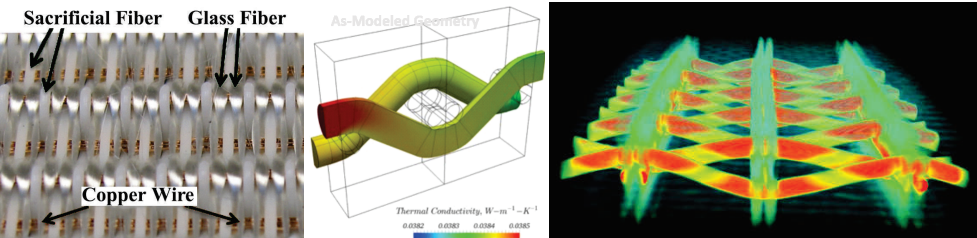


Figure 7. Left: as-woven material, showing the sacrificial fibers, copper wires, and glass fiber spacers; center, showing the as-modeled geometry, and right, showing a micrograph of the as-manufactured channels with a high-contrast liquid.

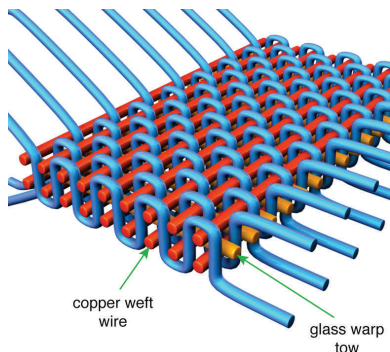


Figure 8. As-woven geometry.

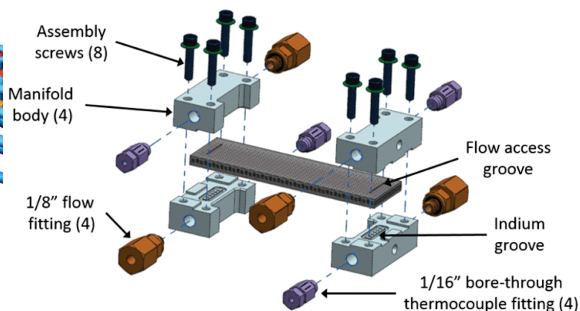


Figure 9. Manifolding of the low- and high-pressure channels

The heat exchanger was manufactured with five pairs of channels with 300 μm diameter, and 50 rows of copper wires. The maximum (ideal) heat exchanger effectiveness would be 98% if each copper wire were to provide perfect exchange between the high- and low-pressure capillaries.

Manifolding was accomplished by CU Aerospace by machining a groove across the sample, which captures alternating channels, as shown in Figure 9. These grooves captured either the top set or the bottom set of capillaries shown in Figure 8. This simple manifolding technique worked well and solved a difficult problem of counterflow heat exchangers (manifolding the two gas streams in a simple and cost-effective way).

The counterflow heat exchanger pressure drop was measured in the high and low pressure channels and is shown in Figure 10. At the nominal flow rate of 15-20 scc/s, the pressure drop was roughly 3 PSI, an acceptably low value, with >98% of the pressure drop predicted to occur at the JT constriction.

Cold Block

The cold block heat exchanger used fine mesh copper screens diffusion-bonded into a block, as shown in Figure 11. The mating piece of the copper block included a constricting capillary 25 mm long and 75 μm ID. The measured flow vs. high pressure is shown in Figure 12. The measured nitrogen flow with 150-200 PSI pressure drop is 18 scc/s, the desired flow for the JT cryocooler.

JT Working Gas

Testing was conducted with R14 gas (CF_4). The boiling point of R14 as a function of pressure is shown in Figure 13, indicating the expected operating pressure is around 175-180 K for a low pressure of 75-100 PSIA. Eventually, gas mixtures will be used to achieve 125-150 K^{7,8}.

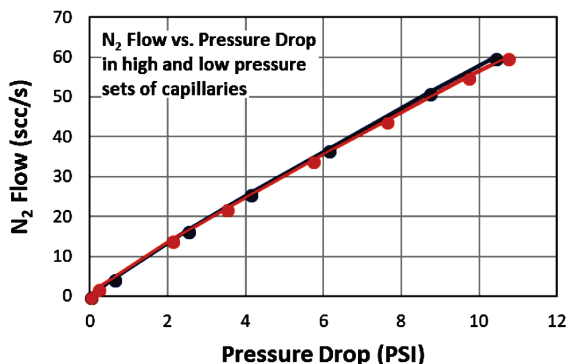


Figure 10. Measured pressure drop in the high and low pressure capillaries.

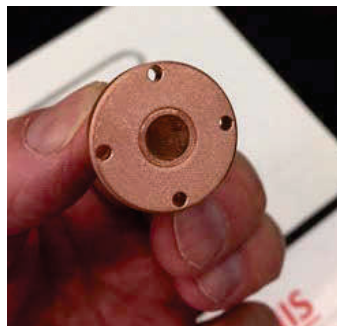


Figure 11. Cold block, showing diffusion-bonded copper screens for heat exchange

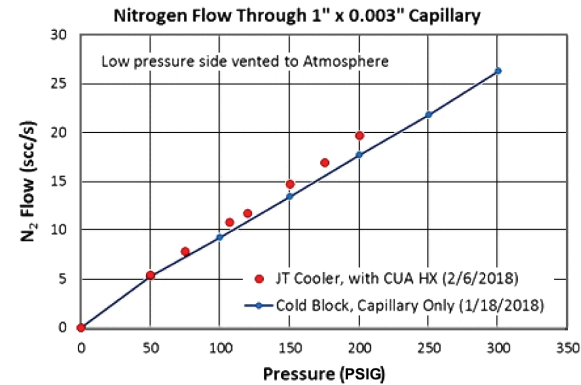


Figure 12. Measured flow through constricting JT capillary.

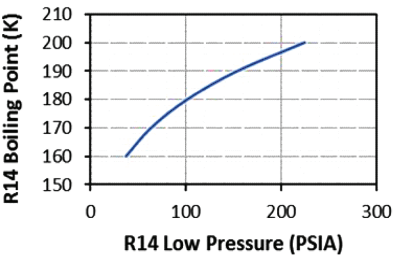


Figure 13. Boiling point of R14 gas as a function of pressure.

JT Cryocooler Test Results

Figure 14 shows the JT coldhead, and shows the coldhead installed in the vacuum chamber and insulated with MLI.

Closed-Cycle JT Testing

For closed-cycle testing, the JT compressor was connected to the inlet and outlet tubes shown in Figure 14. The gas low pressure was measured and set to 100 PSIA. The high pressure was not instrumented, nor were any temperatures other than the cold block temperature, due to budget constraints. The working space was cleaned by flowing high-purity helium gas and periodically pumping on the coldhead. Performance of the closed-cycle cooler is shown in Figure 15, with rather disappointing results. The cold block slowly cooled to around 6 K below ambient temperature. The measured R14 gas flow rate, and the measured compressor input power were consistent with a high pressure in excess of 300 PSI with 100 PSI low pressure.

The high-pressure gas line included no aftercooler heat exchanger, so although none of the hardware ever felt warm, it is possible that the high-pressure gas entering the counterflow heat exchanger was significantly warmer than ambient temperature.

Open-Cycle JT Testing

In order to eliminate the JT compressor as the source of the poor cooler performance in Figure 15, the compressor was removed, the R14 gas bottle was connected to the high-pressure side through a regulator, and the low-pressure side vented to ambient pressure. Testing was performed first with the configuration shown in Figure 12 with a single HX. The high pressure was set to 250 PSIG, and over the course of 6 hours, the cold block cooled to around 27 K below ambient temperature, as shown in the blue curve in Figure 16.



Figure 14. JT coldhead (left), installed in the vacuum can (center) and wrapped in MLI (right).

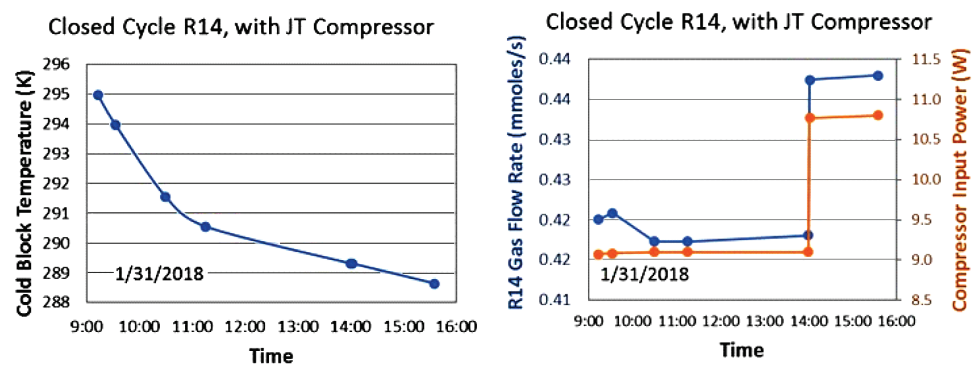


Figure 15. Measured cooldown of closed-cycle JT cryocooler. Temperatures are shown on the left, and measured flow rate and compressor input power are shown on the right.

The slow response led us to install a second identical counterflow heat exchanger in series with the first. A photo of the dual HX configuration is not shown, but measured data are shown in Figure 16, in orange. During testing with the dual HX, the high pressure was held fixed at 250 PSI (red curve), and the R14 gas flow rate was 0.65-0.7 mmoles/s (green curve).

Data Analysis

Although there was no instrumentation of the gas temperatures, it is still possible to estimate the HX effectiveness. The effectiveness is approximately $1 - (dT/\Delta T)$ where dT is the temperature difference between the high- and low-pressure gas streams at the cold end of the HX, and ΔT is the temperature difference between the ambient end and the cold end. The dT at the cold end can be estimated from the JT expansion coefficient of R14 gas (0.049 K/PSI and the pressure difference (250 PSI) to be 12.25 K. For the case of the single HX, the measured effectiveness = $1 - 12.25 \text{ K} / 26 \text{ K} = 0.53$. For the case of the dual HX, the measured effectiveness = $1 - 12.25 \text{ K} / 52 \text{ K} = 0.76$. As expected, the ineffectiveness $dT/\Delta T$ scales with $1/N$ where N = the number of heat exchangers. For high cooler efficiency, a heat exchanger effectiveness in excess of 0.95 is required.

CONCLUSIONS AND FUTURE PLANS

Although the test results were disappointing, there were many positive aspects to this Phase II STTR program:

- 1. CU Aerospace was able to design and build a complex anisotropic composite heat exchanger utilizing sacrificial fiber technology.

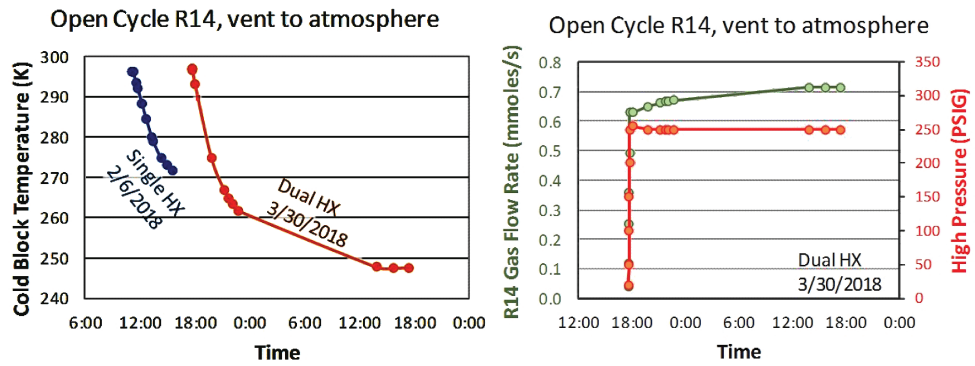


Figure 16. Measured cooldown of open-cycle JT cryocooler. Temperatures are shown on the left, and measured flow rate and high pressure are shown on the right.

2. A clever manifolding technique was devised which solved one of the most challenging problems for any counterflow heat exchanger, manifolding the high- and low-pressure channels.
3. The counterflow heat exchanger did not have any measurable leakage to the environment, even after multiple thermal cycles to cryogenic temperatures.

There is still clearly a need to increase the thermal transfer between the high- and low-pressure channels by utilizing the correct weave between the sacrificial fibers and the copper wires. CU Aerospace has a clear path forward on this task, and we are awaiting additional funding to manufacture and test a heat exchanger with good heat transfer. Thermal modeling indicates that it is possible to achieve an effectiveness in excess of 95% with a single counterflow heat exchanger block.

ACKNOWLEDGMENT

This work was funded by AFOSR STTR Phase II Contract No. FA9550-15-C-0019.

REFERENCES

1. Olson, J.R., Champagne, P., Roth, E. and Nast, T., "JT Micro Compressor Test Results," *Cryocoolers 19*, ICC Press, Boulder, CO (2016), pp. 369-375.
2. Petach, M., Michaelian, M., Nguyen, T. Colbert, R. and Mullin, J., "Mid InfraRed Instrument (MIRI) Cooler Compressor Assembly Characterization," *Cryocoolers 19*, ICC Press, Boulder, CO (2016), pp. 1-8.
3. Adams, A.L., et al., "Infrared focal plane arrays for spectroscopic applications," *Proc. SPIE*, Vol. 7319, (2009).
4. Olson, J.R. et al., "Coaxial Pulse Tube Microcryocooler," *Cryocoolers 18*, ICC Press, Boulder, CO (2014), pp. 51-57.
5. Patrick, J.F., et al., "Robust sacrificial polymer templates for 3D interconnected microvasculature in fiber-reinforced composites," *Composites Part A: Applied Science and Manufacturing*, (2017), pp 361-370.
6. Esser-Kahn, A.P., et al., "Three-Dimensional Microvascular Fiber-Reinforced Composites," *Advanced Materials*, 23(32), (2011), pp. 3654-3658
7. Detlor, J., Pfothenhauer, J. and Nellis, G., "Mixture Optimization for Mixed Gas Joule-Thomson cycle," *IOP Conf. Series: Materials Science and Engineering*, (Vol. 278, No. 1, p. 012045), (2017)
8. Detlor, J. Pfothenhauer, J., Nellis, G., "Experimental Investigation of Mixture Optimization for mixed Joule-Thomson Cycle," *Cryocoolers 20*, ICC Press, Boulder, CO (2018), (this proceeding).